International Journal of Enhanced Research in Science Technology & Engineering, ISSN: 2319-7463
Vol. 3 Issue 2, February-2014, pp: (388-393), Impact Factor: 1.252, Available online at: www.erpublications.com

A Performance Comparison of Dye-Sensitized Solar Cells Based on Mesoporous and Nanostructured Photoanodes

Divya Jyoti[1], Devendra Mohan[2], Amrik Singh[3]
[1]Department of Physics, Punjabi University College, Jaito, Distt. Faridkot, Punjab, India
[2]Laser Laboratory, Department of Applied Physics, Guru Jambheshwar University of Science and Technology, Hisar, Haryana, India
[3]Department of Physics, Chaudhary Devi Lal University, Sirsa, Haryana, India

Abstract: A comparison has been drawn in pure anatase and rutile forms of TiO_2 films with their respective nano crystalline forms as photoanodes in dye-sensitized solar cells. All the films have been synthesized by using sol-gel method. Crystalline nature of the films has been investigated by x-ray diffraction (XRD) and morphologies have been studied by scanning electron microscopy (SEM). The short-circuit current density (J_{SC}) for anatase based cell is about 30% higher than that of rutile based cell. Efficiency values obtained for nano anatase and rutile based DSSCs are 6.6% and 4.8% respectively. The results have been further approved by diffusion coefficient studies which reveal that rutile film has a poor diffusion coefficient than anatase film.

Introduction

Dye-sensitized solar cells (DSSCs) have drawn attention of the researchers as an efficient low-cost alternative to traditional silicon solar cells [1-4]. In DSSC, unbeatable properties of titanium dioxide (TiO_2) viz. appropriate energy levels, dye adsorption ability, low cost, and easy preparation have prompted its used as nano-porous thin film acting as photoanode in DSSCs [5-8]. Intensive research on the photophysics and photochemistry of TiO_2-based DSSCs has shown that the power conversion efficiency of TiO_2 is greatly affected by its particle size, crystalline phase, surface area, film porosity and dye affinity [9-11]. TiO_2 exists in two major allotropic forms: anatase and rutile. The anatase phase (a-TiO_2) has attracted researchers to a great extent because of its more favorable surface chemistry and smaller particles for more dye adsorption [12].

A light harvesting photovoltaic system containing wide band gap semiconductor surface incurres a drawback that monolayer of photosensitizing dye can harvest a very small of light because it absorbs very few light photons. Therefore it becomes necessary to enlarge the interfacial area between the oxide semiconductor layer and the sensitizing dye. This can be successfully accomplished by fabricating nanoparticles based photoelectrodes that enhance the photoactivity [13-18].

Nanomaterials manifest lots of promise primarily due to their wide spectrum of properties that are entirely different from their bulk counterparts [19-23]. In nano phase, the materials have properties entirely different from corresponding bulk phase, therefore it is expected that dye-sensitized solar cells (DSSCs) based on nanocrystalline anatase and rutile will display a drastic change in photovoltaic properties [24]. The photochemical model of photosynthesis can also be applies to describe the operating mechanism of DSSC. According to photochemical model, light selectively excites the molecules which absorb light and causes a transition of electrons from ground level to higher electronic level. The system can now be termed as a combination of ground and excited electronic levels. Quasi chemical potential comes into picture when such a system absorbs radiations. In many systems, such systems are heterogeneous with distinct phases microscopically mixed [25-28].

Experimental

TiO_2 thin films in two different allotropic forms have been synthesized by sol-gel dip coating technique. 3 mL of titanium precursor Titanium iso-propoxide (TTIP) was taken in a flask. 1.26 mL of glacial acetic acid was mixed with 60 mL of ethanol and 1 mL of water and ingratiated with titanium precursor. The solution was stirred for 16 hours in a sealed flask with the help of a magnetic strirrer. Then the solution was refrigerated for 3 days at 4^{O}C. Before executing the coating process, the sol was stirred until it reached at room temperature. Then sol was layered down onto indium tin oxide (ITO) coated glass plates using dip coater (MTI Corporation) at a dipping rate of 5cm/min. ITO coated glass plate was kept there

for 10 minutes and removed at the same rate and then, dried at 120^{O}C for 1 hour. Finally, the annealing of one film was done at 250^{O}C and other at 350^{O}C.

For nanophase formation, 20mL of titanium tetra isopropoxide (TTIP) was poured in a flask and 120mL of 0.1M HNO_3 was mixed drop wise under vigorous stirring for half an hour. The solution was stirred at 80^{O}C for 10 hours. After distributing the solution in two parts, one flask was put in microwave at 180^{O}C for 5 minutes and 1.25mL of isopropanol was mixed in other flask solution and stirred the solution for 30 minutes at room temperature and then kept at 150^{O}C for 6 hours.

The stirring of the solution has been carried out until it reached at room temperature before coating and then deposited on indium tin oxide (ITO) coated glass plates using dip coater (MTI Corporation) at a dipping rate of 8cm/min kept there for 10 minutes and removed at the same rate followed by drying at 125^{O}C for 1 hour. Finally, one film was calcinized at 250^{O}C and other at 550^{O}C.

For the fabrication of DSSC, all the photoanodes were kept immersed in N719 dye and a solution of acetonitrile, lithium iodide and iodine was used as electrolyte.

Results and Discussion

Crystalline structure of films has been confirmed by x-ray diffraction analysis. The x-ray diffraction spectra of an anatase film and of a rutile film have been shown in Figure 1. The broad feature at low angle in the spectra arises from the amorphous substrate. In each spectrum shown in Figure 1, all the diffraction peaks can be indexed in terms of a unique crystalline phase (anatase or rutile). Anatase peaks have been found corresponding to 101, 004, 112, 200, 211, 204, 301 planes and 110, 200 are the rutile planes. Therefore, within the resolution of x-ray diffraction, the single-phase character of synthesized thin films is confirmed. No phase mixing has been observed in any of the two films that is each film retains only single phase.

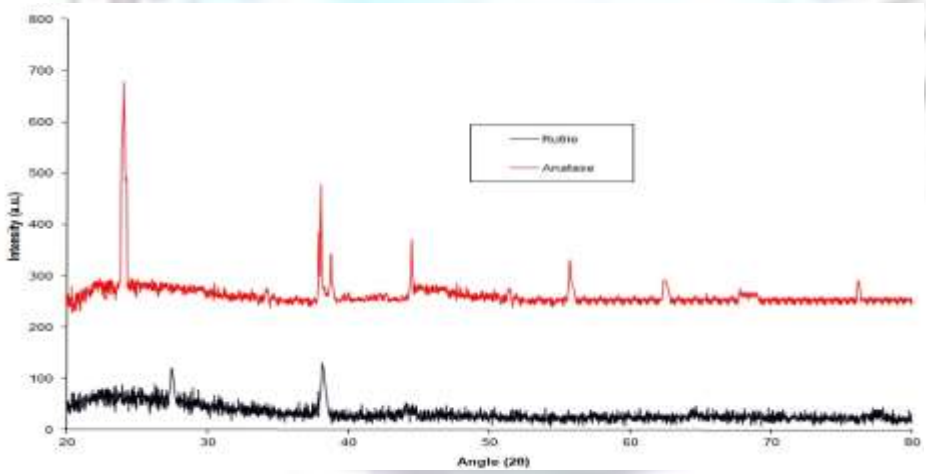

Figure 1. XRD pattern for anatase and rutile films

The XRD plots for nanocrystalline anatase and rutile films have been shown in Figure 2. In each spectrum shown in Figure 2 each diffraction peak corresponds to a unique crystalline phase. Nanocrystalline anatase film contains 101, 103, 004, 112, 200, 105, 211, 204, 116 planes and 110, 101, 111, 211, 002 are the planes possessed by nanocrystalline rutile thin film. Particle sizes for the films are approximately 51.42 nm and 38.12 nm for anatase and rutile films respectively as calculated by Debye scherrer's formula given below [17]:

$$D = \frac{0.9\lambda}{\beta \cos\theta} \qquad (5.13)$$

Here D is average crystallite size, λ represents x-ray wavelength (=0.154 nm in this case), θ be angle of diffraction and β depicts full width at half maximum (FWHM) of diffraction line observed in radians

.

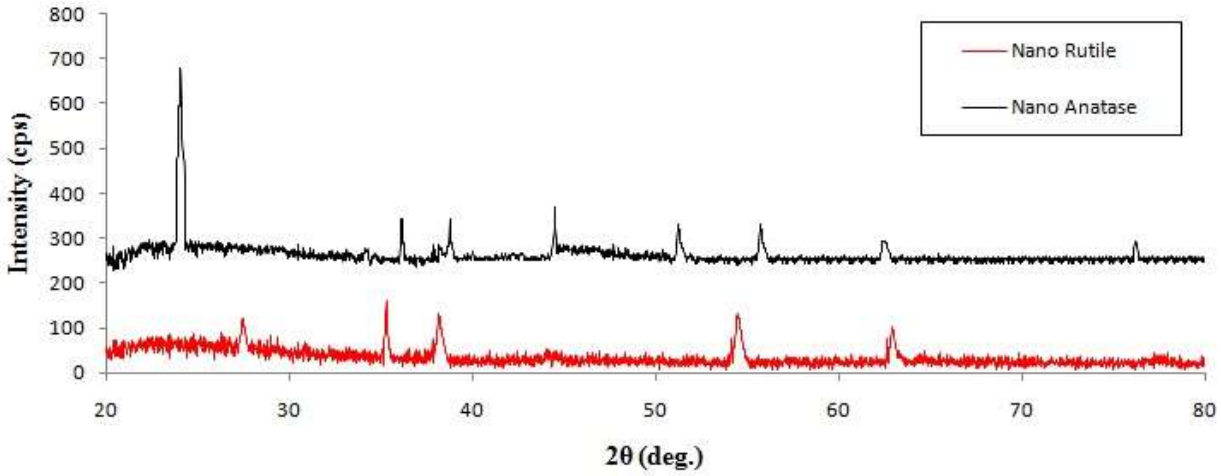

Figure 2. XRD plot for nano anatase and nano rutile

Surface structures of the films have been studied by using scanning electron microscopy (SEM) at e resolution of 500 µm. SEM images revealed that there has been a very narrow particle size distribution of TiO_2 particles (Figure 3). Rough morphology of both the films makes them suitable for larger dye adsorption which is a favorable condition to be used in dye-sensitized solar cells. SEM images clearly indicate that rutile film will hold less number of dye molecules as compared to the film in anatase phase. Less tethering with dye means low concentration of photoelectrons thereby lowering the DSSC output.

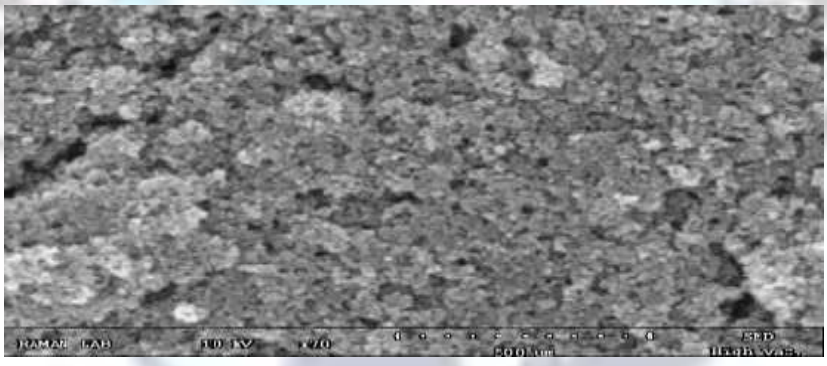

(a)

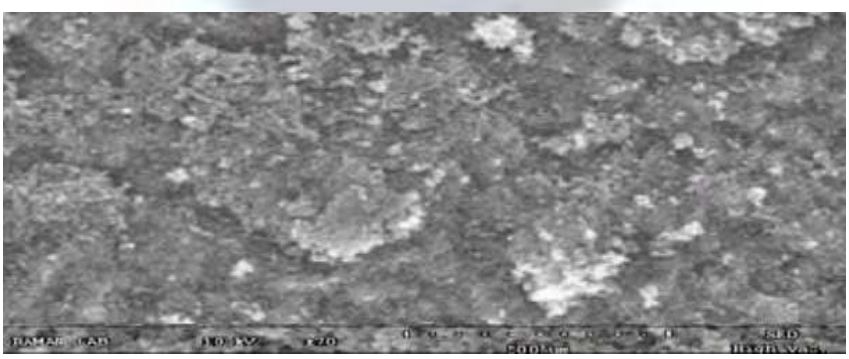

(b)

Figure 3. SEM images of mesoporous TiO_2 (a) anatase and, (b) rutile films

Morphological statuses of the films have been displayed in SEM images (Figure 4) recorded at a resolution of 5 µm. The rough and porous nature of the films has been clearly indicated in the images. SEM images portray the results provided by poroellipsometry i.e. porosity of anatase film is higher (P= 40.4) than that of rutile (P= 35.8).

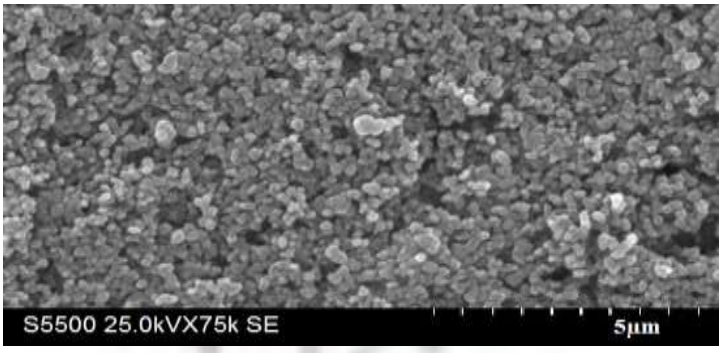

(a)

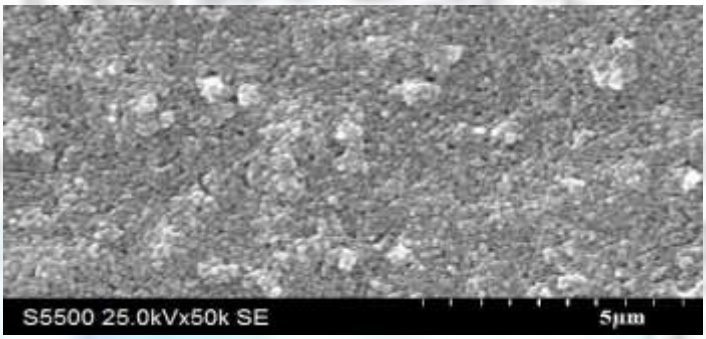

(b)

Figure 4. SEM images for nanocrystalline (a) anatase (b) rutile thin films

The assembled N719 dye sensitized TiO_2 solar cells have been characterized by measuring current density-voltage (JV) curves under standard AM 1.5 simulated sunlight (power density 100W/cm^2). The typical JV curves for the mesoporous film based DSSCs have been shown in Figure 5. It is very well picturized in the figure that open-circuit voltages for the anatase and rutile based dye-sensitized solar cells are nearly same but short–circuit current density values for both are very far from each other. This may be belonging to the slower electron transport in rutile thin films than anatase. Extent of interparticle connectivity associated with particle packing density is lesser in rutile. To withdraw an effective amount of photocurrent from rutile based DSSC, one has to increase surface area of the rutile film by producing a more densely packed structure of smaller particles. Consequently, it can be expected that nanocrystalline rutile films will perform better in DSSC conditions.

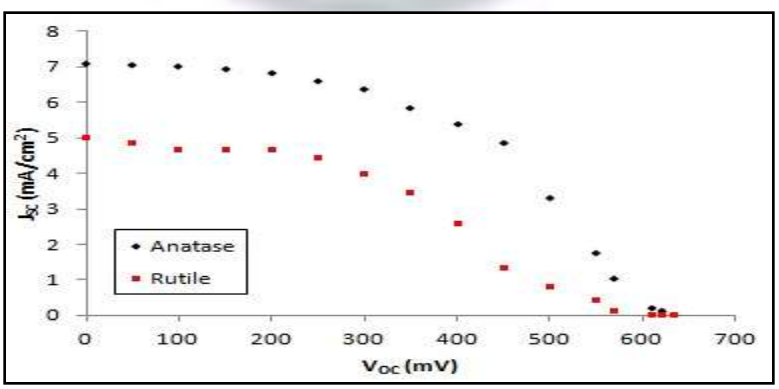

Figure 5. JV curves for anatase and rutile based DSSCs

Open-circuit voltages (V_{OC}) have been found to be 0.633 and 0.621 mV that are not very different from each other but Short-circuit current density (J_{SC}) takes the values 7.1 and 5.0 mA/cm^2 for anatase and rutile based DSSCs respectively. The active area of both the cells is ~ 3cm^2. Efficiencies of the anatase and rutile DSSC came out be 2.18% and 1.21% respectively.

Figure 6 explores JV characteristics of dye-sensitized solar cells based on mesoporous anatase and rutile films. The observed open-circuit voltage (V_{OC}) values for anatase and rutile based cells are 0.73 and 0.72 respectively which are very close. The short-circuit current density (J_{SC}) of rutile based cell (14.05 mA/cm^2) and that of anatase based cell (10.64 mA/cm^2) which is about 30% more than that of rutile based cell. The calculated fill factors are 0.64 and 0.67 for anatase and rutile based DSSCs respectively. The overall efficiencies of the meso-nano anatase and rutile based solar cells are 6.6% and 4.8% respectively.

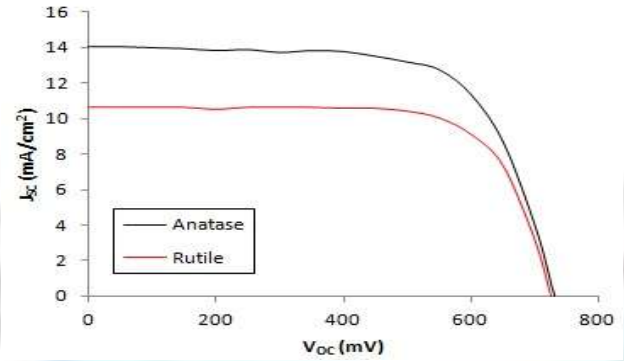

Figure 6. JV characteristics of nanocrystalline anatase and rutile based solar cells

The obtained parameters have been again validated by diffusion coefficient (D_n) calculated by intensity modulated photocurrent spectroscopy (IMPS) using the relation [20]:

$$D_n = \frac{d^2}{4\tau_{IMPS}} \quad (7)$$

here d is the thickness of the thin film and τ indicates the relaxation time of the electrons.

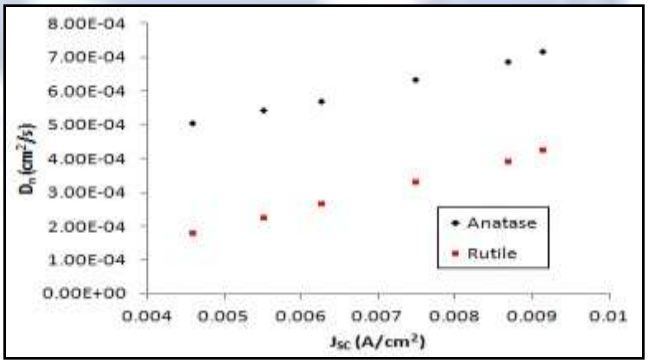

Figure 7. Effective electron diffusion coefficients measured for dye-sensitized anatase and rutile films

Figure 7 unveils the variation in diffusion coefficient of the films with short-circuit current density and it is clear from the plots, for the same value of J_{SC}, diffusion coefficient of rutile film is lower than that of anatase film. And a lesser diffusion coefficient indicates slower electron transport in rutile layer, thereby leading to smaller value of efficiency. Rutile film has a smaller number of interparticle connections per unit film volume than that of anatase film. Thus, the number of routes encountered by an individual electron during its pathway to TCO layer is are lesser than that for anatase. Limiting the number of conducting routes through the network of particles is expected to slow down the transport of electrons through the rutile film and thereby lowering its electron diffusion coefficient.

Conclusions

A comparison of performance of anatase and rutile based DSSC has been made by obtaining JV characteristics. Obtained efficiency values for anatase based and rutile based DSSCs are 2.18% and 1.21% respectively under one sun illumination. Although the V_{OC} values for both the cells are not very much different, but the J_{SC} and hence efficiency values indicate that mesoporous anatase based dye-sensitized solar cell gives comparatively higher output. Thus, anatase is better choice for DSSC photoanode as compared to rutile one. It has been found that nanocrystalline anatase DSSC has a higher efficiency (6.6%) than that of rutile based cell (4.8%). The acquired results have been approved by diffusion coefficient measurements. All the obtained results have realized the performance of allotropic forms of TiO_2 in DSSC framework and inferred that nanocrystalline anatase based dye-sensitized solar cell is a best choice for a competent PV market.

References

[1]. A. Sedghi and H. N. Miankushki, Int. J. Electrochem. Sci. 7: 12078–12089 (2012).
[2]. B. E. Hardin, H. J. snaith and M. D. McGehee, Nature Photonics 6: 162-169 (2012).
[3]. I. Chung, B. Lee, J. He, R. P. H. Chang and M. G. Kanatzidis, Nature 485: 486- 492 (2012).
[4]. Y. S. Jin and H. W. Choi, J Nanosci Nanotechnol. 12(1): 662-667 (2012).
[5]. K. E. JaSiM, Sains Malaysiana 41(8): 1011–1016 (2012).
[6]. A. Yildiza, S. B. Lisesivdin, M. Kasap and D. Mardare, Journal of Non-Crystalline Solids 354: 4944–4947 (2008).
[7]. I. Abayev, A. Zaban, F. Fabregat-Santiago and J. Bisquert, Phys. Stat. Sol. (a) 196(1): R4–R6 (2003)
[8]. Meng Ni, Michael K. H. Leung, Dennis Y. C. Leung, K. Sumathy, Sol. Energy Mater. Sol. Cells 90: 1331 -1344 (2006).
[9]. L. Dloczik, O. Iluperama, I. Lauermann, L. M. Peter, E. A. Ponomarev, G. Redmond, N. J. Shaw, I. Uhlendorf, J. Phys. Chem. B, 101: 10281-10292 (1997).
[10]. T. Matsumura and Y. Sato, J. Mod. Phys. 1: 340-347 (2010).
[11]. A. Yildiz, S. B. Lisesivdin, M. Kasap and D. Mardare, Journal of Non-Crystalline Solids 354: 4944–4947 (2008).
[12]. M. N. Alexander and D. F. Holcomb, Rev. Mod. Phys. 40: 815-829 (1968).
[13]. H. Fritzche and M. Cuevas, Phys. Rev. 119: 1238-1245 (1960).
[14]. N. F. Mott, Adv. Phys. 16: 49-144 (1967).
[15]. N. F. Mott, Can. J. Phys. 34: 1356-1368 (1956).
[16]. A. L. Viet, R. Jose, M. V. Reddy, B. V. R. Chowdary and S. Ramaksrishna, J. Phys. Chem. C 114(49): 21795–21800 (2010).
[17]. Y. Toyozawa, J. Phys. Chem. Sol. 25: 59-71 (1964).
[18]. Y. Zhao, D. W. Brown and K. Lindenberg, J. Chem. Phys. 107(8): 3159-3178 (1997).
[19]. J. Bisquert, D. Cahen, G. Hodes, S. Ruhle and A. Zaban, J. Phys. Chem. B 108: 8106-8118 (2004).
[20]. J. K. Koh, J. Kim, B. Kim, J. H. Kim and E. Kim, Advanced Materials 23(14): 1641-1646 (2011).
[21]. B. E. Hardin, H. J. Snaith and M. D. McGehee, Nature Photonics 6: 162-169 (2012).
[22]. A. Ojala, H. Burckstummer, M. Stolte, R. Sens, H. Reichelt, P. Erk, J. Hwang, D. Hertel, K. Meerholz and F. Wurthner, Adv. Mater. 23(45): 5398-5403 (2011).
[23]. T. Daeneke, T. H. Kwon, A. B. Holmes, N. W. Duffy, U. Bach and L. Spiccia, Nature Chemistry 3: 211-215 (2011).
[24]. Y. Bai, Y. Cao, J. Zhang, M. Wang, R. Li, P. Wang, S. M. Zakeeruddin and M. Gratzel, Nature materials 7: 626-630 (2008).
[25]. S. Q. Fan, C. J. Li, G. J. Yang, L. Zi Zhang, J. C. Gao and Y. Xin Xi, Journal of Thermal Spray Technology 16(56): 893-897 (2007).
[26]. Z. Wei, Y. Yao, T. Huang and A. Yu, Int. J. Electrochem. Sci. 6: 1871 – 1879 (2011).
[27]. M. Riazian and A. Bahari, International Journal of the Physical Sciences 6(15): 3756-3767 (2011).
[28]. S. H. Liu and J. W. Syu, Int. J. Electrochem. Sci 8: 336 – 346 (2013).